

EXPERIMENTAL APPROACHES TOWARDS INTERPRETING DOLPHIN-STIMULATED BIOLUMINESCENCE

JIM ROHR^{1,*}, MICHAEL I. LATZ², STEWART FALLON², JENNIFER C. NAUEN² AND ERIC HENDRICKS¹

¹SPAWARSYSCEN, San Diego, CA 92152-5000, USA and ²Scripps Institution of Oceanography, Marine Biology Research Division, University of California San Diego, La Jolla, CA 92093-0202, USA

*Author for correspondence (e-mail: rohr@nosc.mil).

Accepted 22 January; published on WWW 20 April 1998

Summary

Flow-induced bioluminescence provides a unique opportunity for visualizing the flow field around a swimming dolphin. Unfortunately, previous descriptions of dolphin-stimulated bioluminescence have been largely anecdotal and often conflicting. Most references in the scientific literature report an absence of bioluminescence on the dolphin body, which has been invariably assumed to be indicative of laminar flow. However, hydrodynamicists have yet to find compelling evidence that the flow remains laminar over most of the body. The present study integrates laboratory, computational and field approaches to begin to assess the utility of using bioluminescence as a method for flow visualization by relating fundamental characteristics of the flow to the stimulation of naturally occurring luminescent plankton.

Laboratory experiments using fully developed pipe flow revealed that the bioluminescent organisms identified in the field studies can be stimulated in both laminar and turbulent flow when shear stress values exceed approximately 0.1 N m^{-2} . Computational studies of an idealized hydrodynamic representation of a dolphin (modeled as a 6:1 ellipsoid), gliding at a speed of 2 m s^{-1} , predicted suprathreshold surface shear stress values everywhere on the model, regardless of whether the boundary layer flow was laminar or turbulent. Laboratory flow visualization of a sphere demonstrated that the

intensity of bioluminescence decreased with increasing flow speed due to the thinning of the boundary layer, while flow separation caused a dramatic increase in intensity due to the significantly greater volume of stimulating flow in the wake. Intensified video recordings of dolphins gliding at speeds of approximately 2 m s^{-1} confirmed that brilliant displays of bioluminescence occurred on the body of the dolphin. The distribution and intensity of bioluminescence suggest that the flow remained attached over most of the body. A conspicuous lack of bioluminescence was often observed on the dolphin rostrum and melon and on the leading edge of the dorsal and pectoral fins, where the boundary layer is thought to be thinnest. To differentiate between effects related to the thickness of the stimulatory boundary layer and those due to the latency of the bioluminescence response and the upstream depletion of bioluminescence, laboratory and dolphin studies of forced separation and laminar-to-turbulent transition were conducted. The observed pattern of stimulated bioluminescence is consistent with the hypothesis that bioluminescent intensity is directly related to the thickness of the boundary layer.

Key words: bioluminescence, dinoflagellate, dolphin, laminar flow, plankton, transition, turbulence.

Introduction

The occurrence of bioluminescence is so widespread in the sea that its absence is more remarkable than its presence (Kelly and Tett, 1978). Dinoflagellates are typically the most abundant sources of bioluminescence in coastal waters; at concentrations greater than 100 cells l^{-1} they emit sufficient bioluminescence to highlight moving objects (Morin, 1983). Ship wakes (Bityukov, 1971; Hastings, 1975), submarines (Tarasov, 1956; Staples, 1966), divers (Lythgoe, 1972), seals (Steven, 1950; Williams and Kooyman, 1985) and fish (Harvey, 1952; Hardy, 1956; Morin, 1983) have all been observed to produce bioluminescent signatures. Nocturnally foraging predators may use the bioluminescence inadvertently

stimulated by swimming animals to locate their prey (Hobson, 1966; Mensinger and Case, 1992; Fleisher and Case, 1995). Bioluminescence stimulated by shoals of fish has been used in aerial assessments of pelagic fish stocks (Roithmayr, 1970; Cram and Hampton, 1976).

Accounts in the scientific literature of dolphins moving through 'phosphorescent seas' most often note a conspicuous absence of flow-stimulated bioluminescence on the dolphin bodies. Perhaps the most frequently referenced account of dolphin-stimulated bioluminescence is by Hill (1950), who alludes to an observation by G. A. Steven of only a thin line of bioluminescence in the wake of the dolphin. Steven (1950)

notes that Hill's (1950) description of his observation is not strictly correct; instead of a single line of bioluminescence, he had observed two clean diverging lines of luminescence to stretch behind the dolphin. These narrow lines of bioluminescence in the wake of the dolphin are believed to originate at the ends of the fins and flukes where tip vortices are generated (Webb, 1978). Fitzgerald (1991) made a similar observation, reporting that, although his own swimming motion, at an estimated speed of 0.05 m s^{-1} , produced intense bioluminescence, dolphins approaching him at a speed of approximately 5 m s^{-1} stimulated bioluminescence 'only at the tip vortices at the flukes'. Because bioluminescence at that time was not thought to be stimulated by laminar flow, these descriptions of a lack of flow-induced bioluminescence on the dolphin body have led to inferences that dolphins can maintain laminar flow at high speeds (Hill, 1950; Steven, 1950; Thompson, 1971; Fitzgerald, 1991; Fitzgerald *et al.* 1995). However, it has since been shown in the laboratory that bioluminescence can be stimulated in both laminar and turbulent flows (Latz *et al.* 1994; Rohr *et al.* 1997). Moreover, current power and speed measurements do not support the presence of strictly laminar flow around a dolphin (Lang and Daybell, 1963; Lang and Norris, 1966; Fish and Hui, 1991). Consequently, the conclusions drawn from these inferences need to be re-evaluated.

Curiously, unlike most descriptions reported in the scientific literature, ships' logs are replete with references to bright luminescent displays produced by swimming dolphins (Hobson *et al.* 1981). For example, Lynch and Livingston (1995) refer to dolphins swimming at night beside their vessel as being 'outlined like ghosts'. The artist M. C. Escher's depiction of dolphins enveloped in bioluminescence (Fig. 1A) (Boal *et al.* 1982) became the basis for a woodcut entitled 'Dolphins in a Phosphorescent Sea'. McKinley and Evans sketched the bioluminescence stimulated by Pacific white-sided dolphins (*Lagenorhynchus obliquidens*) swimming at $2\text{--}3 \text{ m s}^{-1}$, as viewed from the underwater observation chamber of the research vessel *Sea See* (Fig. 1B) (Wood, 1973). They observed regions of bright bioluminescence on the body of the dolphins, which have been interpreted as indicating the transition from laminar to turbulent flow (Ridgway and Carder, 1993; Romanenko, 1995).

It is impossible to reconcile the various accounts of dolphin-stimulated bioluminescence because of the unknown natural conditions and uncontrolled observational circumstances. Factors that may affect the observations include the abundance of plankton species, the physiological responses of the luminescent organisms, ambient lighting, dark adaptation of the eyes of the observer and properties of the stimulating flow field related to dolphin swimming mode. Nonetheless, the possibility of using naturally occurring bioluminescence under controlled conditions is particularly attractive because conventional flow-visualization techniques such as dye, bubbles and particles have proved ineffective for visualizing the flow field around large moving animals in their natural environment (Rosen, 1963; McCutchen, 1976). Luminescent

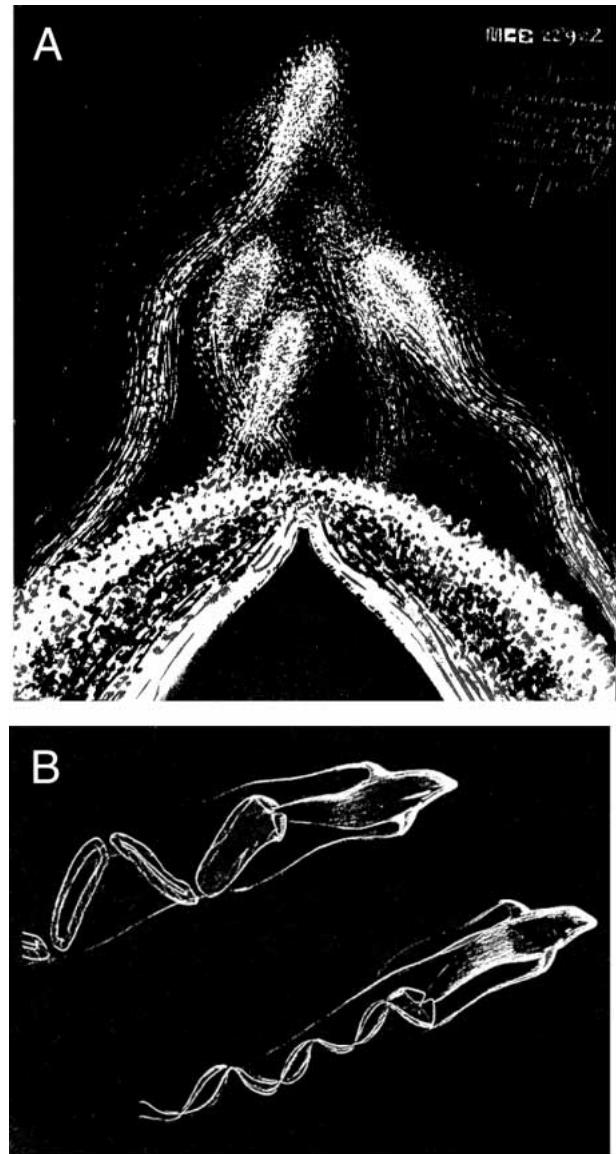


Fig. 1. Previous depictions of dolphins swimming through 'phosphorescent seas' which illustrate flow-induced bioluminescence occurring on the animal. (A) 1922 drawing by M. C. Escher (reproduced with permission). (B) Sketch by L. E. McKinley and W. E. Evans made in 1967 (reproduced with permission).

dinoflagellates are ideal flow markers because they are nearly neutrally buoyant and are slow swimmers. Some species, such as *Lingulodinium polyedrum* (= *Gonyaulax polyedra*), have cells that are similar in size to particles used in conventional tracer methods such as hydrogen bubbles in water (Irani and Callis, 1973). Laboratory studies have successfully demonstrated the feasibility of using the flashes of *L. polyedrum* as a flow marker (Latz *et al.* 1995). With only a 20 ms latency in the response to a mechanical stimulus (Widder and Case, 1981), the near-instantaneous luminescent response of dinoflagellates makes them suitable for flow visualization of fast-moving animals such as dolphins. Throughout the dolphin

speed range of interest, dinoflagellate-sized particles are expected to have no measurable effect on the flow (Ladd and Hendricks, 1985).

The present study includes the first methodical approach towards using bioluminescence for visualizing boundary-layer flow on a dolphin. The boundary layer is defined as the region where the mean flow velocity is less than 99.5 % of that in the free stream (Young, 1989). This study was designed (1) to 'calibrate' luminescent plankton as flow markers by determining their response to quantifiable levels of flow stimuli, (2) to test luminescent plankton as flow-visualization markers by observing their response in flow around laboratory hydrodynamic models, (3) to use numerical simulations to make conservative estimates of the flow stimulus levels on and around a rigid idealized dolphin shape, and (4) to record video images of flow-induced bioluminescence of unrestrained dolphins gliding in natural compositions of luminescent plankton of different species abundance and under various ambient lighting conditions. The present data demonstrate that many of the previous flow inferences based on bioluminescence stimulation are inaccurate and suggest a new interpretation for flow on the body based on the boundary layer thickness.

Materials and methods

Luminescent organisms

Bioluminescence by dinoflagellates exhibits a circadian rhythmicity, with emission 100 times brighter at night than during the day (Sweeney, 1981). Therefore, luminescent organisms for the laboratory experiments were obtained by surface bucket collection approximately 2 h before dusk when bioluminescence is minimally excitable; both laboratory and field measurements were performed several hours into the night phase when maximal levels of bioluminescence occur (Biggley *et al.* 1969). Water samples were preserved in a solution of 1 % glutaraldehyde/1 % paraformaldehyde. To

determine species abundance, 10 or 25 ml samples were poured into a settling chamber (Aquatic Research Instruments) and allowed to settle for a minimum of 2 h and up to 24 h; no differences in counts were noted between the different settling times. Total numbers of organisms were counted at 100× magnification using an inverted microscope. The bioluminescent organisms identified in water samples collected throughout this study were exclusively dinoflagellates, specifically *Lingulodinium polyedrum* (= *Gonyaulax polyedra*) Stein, *Ceratium fusus* (Ehrenberg) Dujardin, *Protoperidinium* spp. and *Noctiluca scintillans* (Macartney) Ehrenberg (Table 1). These luminescent plankton are common to the coastal waters of southern California (Sweeney, 1963; Holmes *et al.* 1967; Kimor, 1983; Lapota *et al.* 1994). The distribution of luminescent plankton in the ocean is both temporally and spatially patchy (e.g. Kelly, 1968; Lapota *et al.* 1994). It was common to measure twofold differences in dinoflagellate cell concentration in consecutive samples taken from the dolphin pen owing to both patchiness and sampling statistics. In the laboratory study, sampling differences were reduced to approximately 20 % variation by gently stirring the contents of the head tank of the experimental apparatus prior to testing. Observations confirmed that the stirring did not stimulate bioluminescence.

The most prevalent bioluminescent species present, *Lingulodinium polyedrum* (Table 1), emits approximately 10^8 quanta (=photons) per flash at a spectral emission maximum of 470 nm (Biggley *et al.* 1969), with each 0.1 s duration flash exhibiting simple exponential decay of light emission (Latz and Lee, 1995). Unlike other dinoflagellates that can produce up to 25 flashes per cell, each *L. polyedrum* cell emits only one or two flashes during its night phase (Latz and Lee, 1995). The bioluminescent potential of the sea water was calculated as the sum of the estimated light contribution from each dinoflagellate species, calculated as the product of the abundance of each species (or taxon) and the corresponding light emission per cell. Values for light emission per cell were

Table 1. Abundance and bioluminescence potential of luminescent dinoflagellates collected during the dolphin video recordings

Dinoflagellate	Cell size (μm)	Bioluminescence potential (quanta cell ⁻¹)	Cell abundance (cells l ⁻¹)			
			Dolphin pen 30/5/94	Dolphin pen 2/6/94	Dolphin pen 11/7/95	Dolphin coastal 1/2/95
<i>Lingulodinium polyedrum</i>	40	10 ^{8a}	2532	1063	1040	36 900
<i>Ceratium fusus</i>	340×30	5×10 ^{8b}	376	180	120	560
<i>Protoperidinium</i> spp.	70×60	3×10 ^{9c}	60	83	100	506
<i>Noctiluca scintillans</i>	800	9×10 ^{10d}	100	30	0	777
Total bioluminescence potential (quanta l ⁻¹)			9.6×10 ¹²	3.1×10 ¹²	0.5×10 ¹²	75.4×10 ¹²
Quality of video images			Good	Poor	Poor	Excellent

Bioluminescence potential was estimated from previous studies where cells were mechanically stimulated until bioluminescence was depleted: ^aBiggley *et al.* (1969); ^bEsaías *et al.* (1973); ^cLapota *et al.* (1989); ^dBuskey *et al.* (1992).

Representative cell size is expressed as length × width or as cell diameter.

obtained from previous studies where individual species were mechanically stimulated to exhaustion (Biggley *et al.* 1969; Esaias *et al.* 1973; Lapota *et al.* 1989; Buskey *et al.* 1992).

Pipe flow 'calibration' of luminescent organisms

Laboratory experiments were conducted simultaneously with field flow-visualization experiments to determine threshold response levels for bioluminescence, the maximum intensity of individual flashes and differences in the response of individual luminescent organisms for laminar and turbulent flows. Fully developed pipe flow was chosen to investigate the response of luminescent organisms because the flow field is well-characterized (Laufer, 1954; Schlichting, 1979). The mean axial velocity profile in fully developed pipe flow remains constant downstream because there is a balance between pressure and shear forces. Shear stress is considered to be the most important flow parameter responsible for bioluminescence (Anderson *et al.* 1988; Latz *et al.* 1994; Rohr *et al.* 1997). For fully developed pipe flow, the profile of shear stress throughout the pipe is determined directly from measurements of pressure drop. Regardless of whether the flow is laminar or turbulent, shear stress decreases linearly from a maximum at the pipe wall, τ_{wall} , to zero at the center line (Bakhmeteff, 1936). The mean shear stress throughout the pipe is two-thirds of τ_{wall} .

It has also been proposed that the length scales of turbulence affect the luminescent response of the organisms (Rohr *et al.* 1990; Widder *et al.* 1993). The range of eddy scales can be estimated in fully developed turbulent pipe flow (Davies, 1972; Rohr *et al.* 1994). The largest turbulent length scales are the size of the pipe radius, while the smallest are of the order of the Kolmogorov scale, defined as $(\nu^3/\epsilon)^{1/4}$, where ν is kinematic viscosity and ϵ is the rate of energy dissipation per unit mass. Deformation of the cell should be most affected by eddies with length scales smaller than the cell diameter.

The pipe flow apparatus (Rohr *et al.* 1990, 1997) consisted of a 75 l acrylic head tank, a gently contracting inlet section and a vertically oriented 0.635 cm i.d. clear polycarbonate pipe fitted with pressure taps. The mean flow velocity through the pipe was determined by weighing the amount of water collected over a measured time and dividing by the pipe cross-sectional area. The pressure drop along the pipe was measured using a variable-reluctance differential transducer (Validyne Corporation). Calculations of mean velocity and wall shear stress confirmed that the cells were in fully developed flow when the measurements of bioluminescence were made (Fig. 2). Sea water collected during the day from the dolphin pen was tested in the pipe flow apparatus the same night after the collection of video data.

Bioluminescence was measured using an RCA 8575 photon-counting photomultiplier tube (PMT) located 67 cm from the pipe inlet in fully developed flow. The field of view of the PMT encompassed the entire width of the pipe and 5.0 cm of length. A typical dinoflagellate flash, lasting between 0.1 and 0.2 s (Anderson *et al.* 1988; Latz and Lee, 1995), resulted in streaks of bioluminescence less than 25–50 cm long at the highest flow

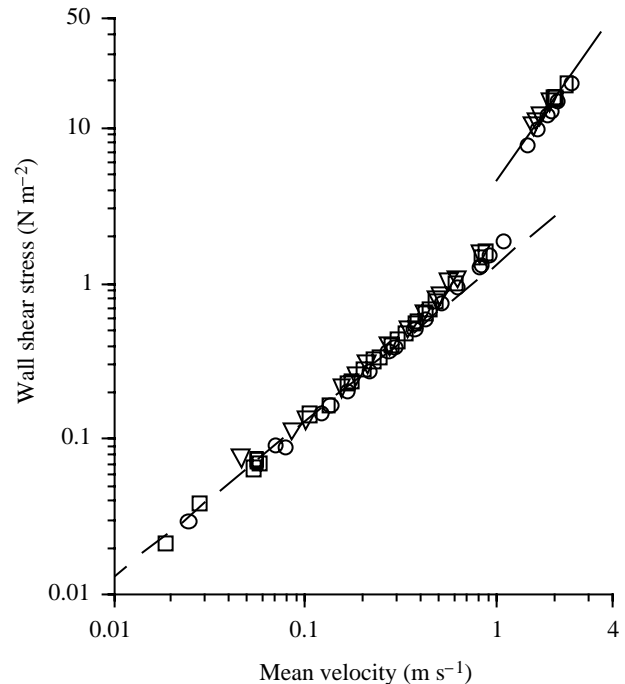


Fig. 2. Relationship between wall shear stress and mean velocity for pipe flow. The dashed line is the theoretical relationship for laminar flow; the solid line is the accepted empirical relationship for turbulent flow (Schlichting, 1979). Data are from experiments performed on 30/5/94 (squares), 2/6/94 (triangles) and 11/7/95 (circles).

rates measured. Consequently, flashes initiated around the pipe inlet where the flow field was not fully developed decayed before reaching the downstream position of the PMT. Bioluminescence time series, composed of consecutive 0.005 s integrations for periods of 20–100 s, were collected at constant flow rates. Mean bioluminescence intensity was obtained by averaging the light emission per second over each time series. Maximum bioluminescence intensity was determined by obtaining the highest value in each bioluminescence time series. Comparison of optically filtered and unfiltered PMT signals established that the intensity of the bioluminescence was not saturating the detectors. Bioluminescence measurements were repeated at similar flow rates throughout each experiment to check whether an uneven cell distribution throughout the tank was influencing data trends.

Laboratory flow visualization

Laboratory bioluminescence flow-visualization experiments with freshly collected samples of mixed plankton (predominantly *Lingulodinium polyedrum*) were performed as an aid towards interpreting field recordings of flow-induced bioluminescence. Experiments were repeated for both high (approximately 500 cells ml⁻¹) and low (approximately 10 cells ml⁻¹) concentrations of luminescent organisms. The laboratory apparatus consisted of a vertical water tunnel, 7.62 cm in diameter, with a 180 l head tank. A 2.54 cm diameter

sting-mounted sphere was used as the test model. To study the effect of forced transition from laminar to turbulent flow on the response of the luminescent organisms, a 0.16 cm thick, 1.1 cm diameter O-ring was placed on the front face of the sphere. Calculation of the Reynolds number of the sphere, $Re_D = U_{\text{mean}}D/\nu$, was based on the mean flow rate U_{mean} , the diameter of the sphere D and the kinematic viscosity of the fluid ν . Shear stresses on the sphere were not calculated because the free-stream flow around the sphere was influenced by the wall of the water tunnel. The effects of cell concentration, boundary layer thickness, flow separation and forced transition from laminar to turbulent flow were examined.

An intensified silicon intensified target (ISIT) video camera (Cohu Inc., model 5162) was used for all laboratory and field work. Images of flow-induced bioluminescence were taken from individual frames of the video record. Except for the absence of color, they are fairly representative of what was observed by the unaided, dark-adapted eye. The video camera was operated at 30 frames s^{-1} in automatic gain and high-voltage control modes. While this setting provided maximum sensitivity, approximately $7 \times 10^{-5} \mu W cm^{-2}$ at a wavelength of 470 nm, it did not provide an absolute index of light intensity. Thus, quantitative comparisons between different images were not possible. A similar constraint is shared by the human eye which, while being a very sensitive photodetector, can only provide a measurement of light by comparison with a source of known intensity (Tett and Kelly, 1973).

Numerical simulation

When Gray (1936) first estimated the surface shear stress on a swimming dolphin, he approximated the surface as a flat plate. A better approximation of the shape of a gliding dolphin is to model it as a rigid 2.42 m long, 6:1 (length to width) ellipsoid (Lang and Daybell, 1963; Norris, 1965), which is the shape modeled in the present study. The numerical model is not intended to simulate the complex motion of an actively swimming dolphin. Rather, it provides the most conservative estimate of surface shear stress on and around the dolphin body while it is gliding. This information, together with the laboratory quantification of shear stress thresholds for plankton luminescence, allows for a conservative prediction of whether the flow around a gliding dolphin could possibly be stimulatory to luminescent dinoflagellates.

Shear stress values on the body (τ_{body}) and in the boundary layer (τ) of the ellipsoid were calculated according to the

numerical scheme of Cebeci and Smith (1974) using Transition Analysis Program System (TAPS) software obtained from McDonnell Douglas. This scheme employs the boundary layer and continuity equations to solve for pressure and axial and radial velocity components throughout the flow. In turbulent flow, Cebeci and Smith (1974) treat the boundary layer as a composite layer characterized by inner and outer regions, each with a separate expression for the eddy viscosity. This method has been remarkably successful in calculating axisymmetric boundary layers around airfoils and torpedo-shaped bodies in incompressible flows (Murphy, 1954; Cornish and Boatwright, 1960). The calculations did not continue to the end of the body because the flow eventually separates and the numerical simulation breaks down. Reynolds numbers were calculated on the basis of the ellipsoid length, L .

Speeds representative of cruising and burst swimming were considered. The lower speed of 2 m s^{-1} ($Re_L = 4.8 \times 10^6$) is a typical cruising speed of the Atlantic bottlenose dolphin *Tursiops truncatus* (Williams *et al.* 1993) and representative of the dolphin speeds recorded during the field study. The higher speed of 8 m s^{-1} ($Re_L = 1.9 \times 10^7$) is characteristic of the burst speeds observed for this species (Lang and Norris, 1966; Lang, 1975; J. Rohr, unpublished data). For the sake of comparison, at each speed, various locations on the ellipsoid were chosen for laminar-to-turbulent transition. The most posterior transition location was set at 2.05 m from the tip of the ellipsoid. This is the position where natural transition is expected to occur for a speed of 2 m s^{-1} on the basis of empirical studies (Smith and Gamberoni, 1956; Van Ingen, 1956; Young, 1989). The most anterior transition location was 0.125 m from the tip of the ellipsoid, roughly equivalent to the apex of the melon.

Dolphin flow visualization

Night-time video images of three adult Atlantic bottlenose dolphins, *Tursiops truncatus* Montegu, were obtained under different ambient light conditions, cell concentrations and assemblages of luminescent dinoflagellates (Table 1). Data are presented for only two animals, identified as NAY and FLP, because natural levels of bioluminescence were too dim to be useful for flow visualization of the third animal. Information on animal size, swimming speed and Reynolds number is listed in Table 2. Reynolds numbers for the moving dolphin were based on animal length, L . The dolphins were housed within floating pens (9.1 m \times 9.1 m \times 3.3 m deep) in San Diego Bay,

Table 2. Characteristics of the bottlenose dolphins (*Tursiops truncatus*) used in the field experiments

Identification	Location	Gender	Age (years)	Mass (kg)	Length (m)	Girth (m)	Speed (m s^{-1})	Re_L
NAY	Open waters	Male	11	204	2.67	1.37	1.0	2.6×10^6
FLP	Pen	Male	16	157	2.41	1.20	2.2	5.1×10^6

Girth was measured at the caudal insertion of the pectoral fin.

Re_L , Reynolds number based on animal length.

where water temperature typically varies between 14 and 21 °C during the year. Animals were fed 2–3 times daily on a vitamin-supplemented diet of mackerel, herring and smelt, and were trained using a positive reinforcement schedule.

Video recordings of the dolphin NAY were made at night from a 5.5 m boat in open waters just outside San Diego Harbor. The dolphin was trained to swim approximately 4 m off the starboard side of the boat. Boat speed was limited to between 0.5 and 1.0 m s^{-1} , because at higher speeds the bioluminescence produced by the boat wake obscured that stimulated by the dolphin. At this low boat speed, NAY appeared to be gliding during most of the video recordings. To study the effect of flow separation, NAY swam with a cylinder (6.5 cm diameter by 2 cm high, axis of cylinder perpendicular to the dolphin surface) attached, *via* a Velcro strap, to the pectoral fin. Recordings were made during red-tide conditions when concentrations of *Lingulodinium polyedrum* were particularly high, for a range of ambient light conditions created by the phase of the moon and background shore light.

Video recordings of FLP were made under controlled conditions in San Diego Bay. FLP was trained to respond to an acoustic signal by swimming between adjacent floating pens through a 1.7 m \times 1.0 m open gate near the water surface. The receiving pen was covered by an opaque tent that made the enclosed area suitably dark for low-light imaging. The animal was acclimated several days prior to filming to swim into the darkened enclosure. A single ISIT video camera operating at 30 frames s^{-1} was located in the darkened pen approximately 1 m above and forward of the entrance gate, providing a dorsal view of the animal. Observations made during the day confirmed that FLP glided through the gate. In order to assess the effect of the latency of the plankton response on the observed pattern of bioluminescence on the dolphin body, a Velcro strap or inverted cup was placed on the rostrum to force transition to turbulent flow or cause flow separation, respectively. Forty-four passes were recorded over two consecutive nights. Particle-tracking methods were not used to analyze the video record for several reasons. In order to view all or most of the dolphin, the camera was too far away to resolve individual flashes. Even at closer ranges, the high concentration and short duration (3–4 video frames) of flashes would preclude their tracking. However, with suitable cell concentrations and viewing distance, and by using organisms with a much longer flash duration, individual bioluminescent flashes have been effectively used for laboratory flow visualization (Latz *et al.* 1995).

Results

Pipe flow 'calibration' of luminescent organisms

The response threshold for flow-stimulated bioluminescence always occurred in laminar flow at $\tau_{\text{wall}} \approx 0.1 \text{ N m}^{-2}$ (Fig. 3). Mean bioluminescence intensity increased with increasing τ_{wall} throughout laminar flow (Fig. 3A). Over the short turbulent range measured, levels of mean bioluminescence continued to increase with τ_{wall} but at a lower rate. Maximum

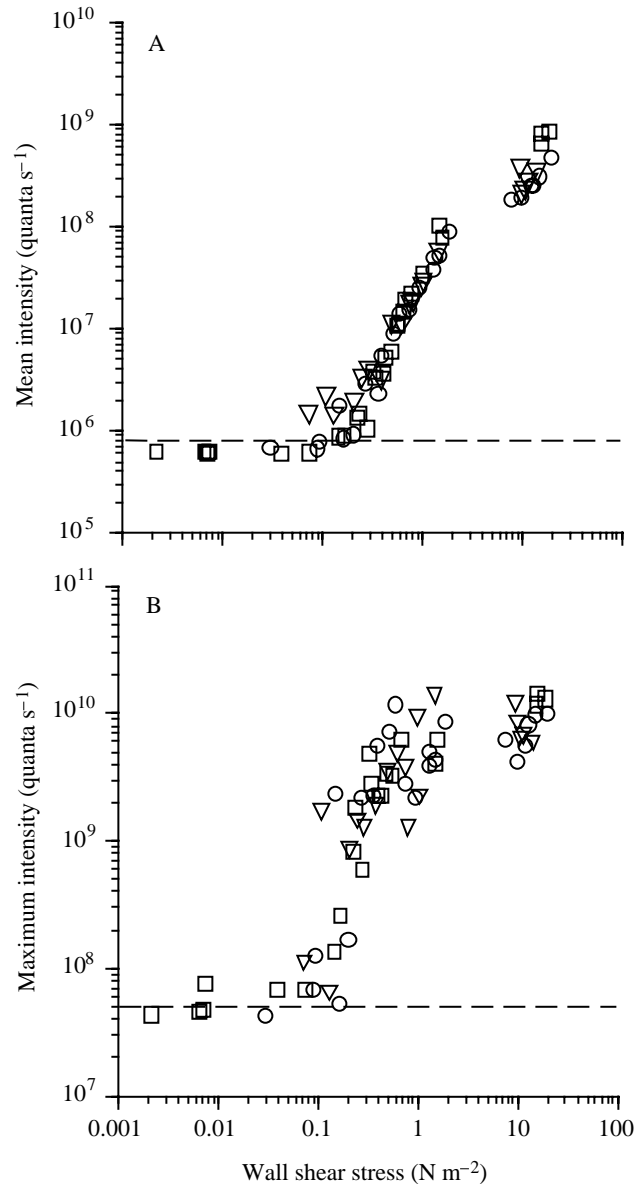


Fig. 3. Bioluminescence intensity as a function of pipe wall shear stress. (A) Mean intensity. (B) Maximum intensity. Experiments were performed on 30/5/94 (squares), 2/6/94 (triangles) and 11/7/95 (circles). Laminar flows had a wall shear stress (τ_{wall}) of less than 2 N m^{-2} . The gap between 2 and 8 N m^{-2} marks the transition from laminar to turbulent flow. The dashed lines represent background light levels when no bioluminescence was stimulated.

bioluminescence intensity per cell exhibited greater variability than mean bioluminescence measurements, because of the low statistical likelihood of a cell being positioned in view of the detector during the short (10 ms) temporal peak of its flash. At low flow rates and organism concentrations, few organisms were stimulated, decreasing the likelihood that the maximum flash intensity would occur in view of the detector, although the low flow speed increases the likelihood that the brightest part of the flash would be measured. At high speeds and cell

concentrations, multiple flashes were simultaneously present within the field of view of the PMT, leading to an artificially high value of maximum intensity. Nevertheless, several trends in the maximum bioluminescence intensity data were evident (Fig. 3B). The intensity of individual flashes appeared generally to increase with τ_{wall} from threshold to approximately 1.0 N m^{-2} . For τ_{wall} values greater than approximately 1.0 N m^{-2} , maximum bioluminescence levels for all the pipe flow experiments were generally similar, suggesting that a maximum organism response had been reached. Remarkably, the maximum response for τ_{wall} values greater than approximately 1.0 N m^{-2} was similar for both laminar and turbulent flows, even when the Kolmogorov scale in turbulent flow was of the order of the *L. polyedrum* cell size.

Laboratory flow visualization

The level of bioluminescence stimulated by flow around the sphere was a function of flow rate, the cell concentration of luminescent organisms and the thickness of the boundary layer. As the flow rate was slowly increased, bioluminescence was first observed on the forward face of the sphere where the shear stress was greatest (Fig. 4A). Streaks of bioluminescence, delineating the trajectory of individual cells, showed the boundary layer separating at the shoulder of the sphere. At higher flow rates, bioluminescence appeared to decrease around the forward face of the sphere, where the boundary layer was thinning, and became most prominent in the wake of the sphere, where the excitation volume was greatest (Fig. 4B).

The concentration of luminescent organisms present in the flow, particularly at low flow rates, also affected the brightness of the observed bioluminescence. At $Re_D \approx 1700$, a cell concentration of approximately 10 cells ml^{-1} resulted in minimal bioluminescence (Fig. 4C), whereas at a cell concentration of approximately $500 \text{ cells ml}^{-1}$ the boundary layer and wake of the sphere were clearly observed (Fig. 4D). At higher Reynolds numbers, a similar pattern of wake structure behind the sphere was readily discerned for both concentrations, although the images were not equally bright (Fig. 4B,E). For similar flow and cell concentrations, forcing transition from laminar to turbulent flow using an O-ring placed at the leading edge of the sphere resulted in a pronounced increase in bioluminescence immediately behind the O-ring (Fig. 4E,F).

Numerical simulation

Surface shear stress values predicted on the ellipsoid (Fig. 5A), for speeds of 2 and 8 m s^{-1} , were always greater than threshold levels for bioluminescence stimulation, regardless of whether the flow was laminar or turbulent. At a speed of 2 m s^{-1} ($Re_L = 4.8 \times 10^6$), the mean τ_{body} over the ellipsoid surface was approximately 1.9 N m^{-2} for mostly laminar flow (natural transition occurred at 2.05 m) and 7.2 N m^{-2} for mostly turbulent flow (forced transition at 0.125 m) (Fig. 5B). When transition was forced at the 0.125 m location, τ_{body} increased by a factor of approximately two at that location. At a speed of 8 m s^{-1} ($Re_L = 1.9 \times 10^7$, data not shown) and forced transition

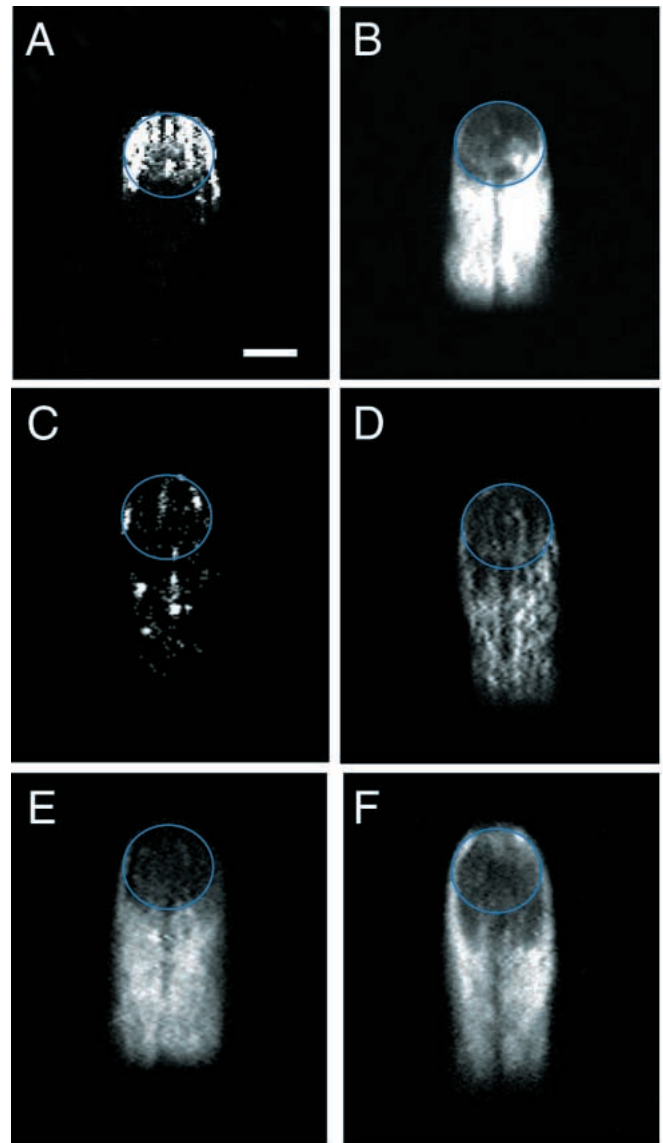


Fig. 4. Images of the bioluminescence of the dinoflagellate *Lingulodinium polyedrum* stimulated by flow around a 2.54 cm diameter sphere for different flow rates (A,B) and cell concentrations (C,D) and for forced transition from laminar to turbulent flow (E,F). Each image represents a single video frame. The blue line outlines the position of the sphere. (A) $U_{\text{mean}} \approx 0.7 \text{ cm s}^{-1}$ ($Re_D \approx 170$), cell concentration $\approx 500 \text{ ml cells}^{-1}$. (B) $U_{\text{mean}} \approx 27 \text{ cm s}^{-1}$ ($Re_D \approx 6600$), cell concentration $\approx 500 \text{ cells ml}^{-1}$. (C) Cell concentration $\approx 10 \text{ cells ml}^{-1}$, $U_{\text{mean}} \approx 7.0 \text{ cm s}^{-1}$ ($Re_D \approx 1700$). (D) Cell concentration $\approx 500 \text{ cells ml}^{-1}$, $U_{\text{mean}} \approx 7.0 \text{ cm s}^{-1}$ ($Re_D \approx 1700$). (E) No forced transition, $U_{\text{mean}} \approx 25 \text{ cm s}^{-1}$ ($Re_D \approx 6200$), cell concentration $\approx 10 \text{ cells ml}^{-1}$. (F) Forced transition, $U_{\text{mean}} \approx 27 \text{ cm s}^{-1}$ ($Re_D \approx 6600$), cell concentration $\approx 10 \text{ cells ml}^{-1}$. Scale bar in A, 1.5 cm. U_{mean} , mean flow rate; Re_D , Reynolds number based on the diameter of the sphere.

at 0.125 m, the calculated mean τ_{body} was 87.5 N m^{-2} . Forced transition resulted in an increase in τ_{body} by a factor of approximately three at the 0.125 m transition location. Where

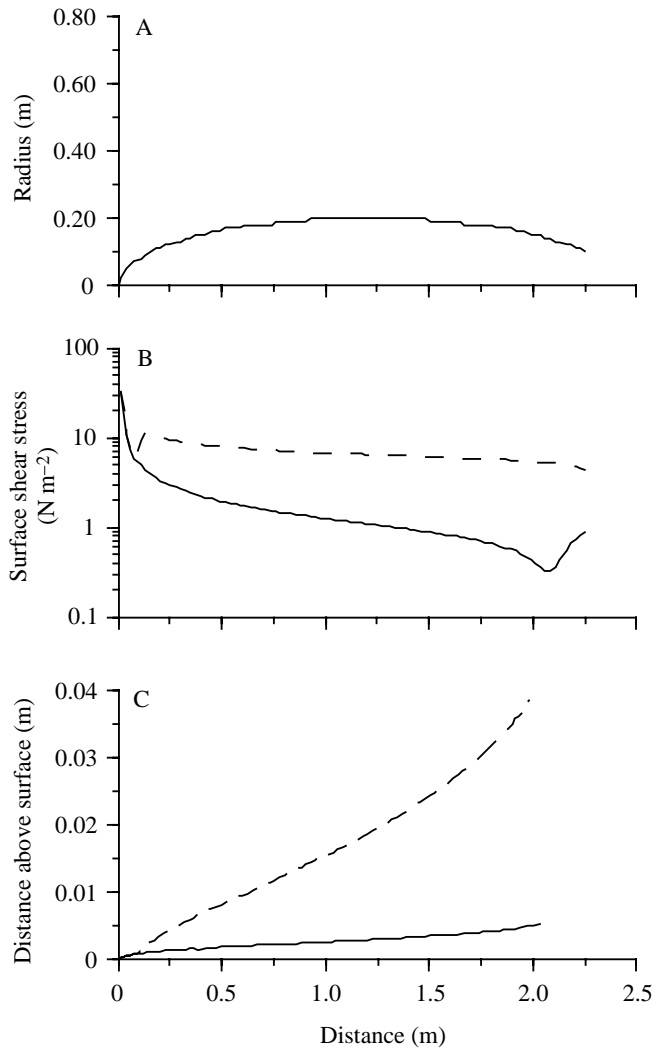


Fig. 5. Results of numerical calculations for a flow of 2 m s^{-1} ($Re_L = 4.8 \times 10^6$) around a 6:1 ellipsoid. (A) Surface profile of the ellipsoid as a function of distance along the body, with center line at a radius of 0. (B) Surface shear stress as a function of distance along the body. (C) Boundaries of the flow along the body where shear stress levels are 0.1 N m^{-2} or greater. The 0.1 N m^{-2} shear stress contour serves as a good approximation of the boundary layer thickness. For B and C, the dashed line represents turbulent flow (transition was forced at 0.125 m) and the solid line represents laminar flow until natural transition occurred at 2.1 m. Re_L , Reynolds number calculated using ellipsoid length L .

natural transition was calculated to occur at 0.5 m for a flow speed of 8 m s^{-1} , τ_{body} increased almost sevenfold at the point of transition and averaged 75.1 N m^{-2} over the body.

For a given cell abundance, the intensity of bioluminescence is related to the volume of flow within which shear stress levels are sufficient to stimulate a response. Over the computational region of interest (prior to separation), the calculated shear stress, τ , decreases monotonically from the surface of the ellipsoid into the free-stream flow. Consequently, the $\tau \approx 0.1 \text{ N m}^{-2}$ contour approximately

Table 3. Numerical calculations of the flow volume around a 6:1 2.41 m long ellipsoid where two levels of shear stress are exceeded

Transition location		Flow volume (m^3)			
		$\tau > 0.1 \text{ N m}^{-2}$		$\tau > 1 \text{ N m}^{-2}$	
(x/L)	x (m)	2 m s^{-1}	8 m s^{-1}	2 m s^{-1}	8 m s^{-1}
0.05	0.125	0.0515	0.0472	0.0311	0.0355
0.10	0.250	0.0490	0.0449	0.0298	0.0339
0.21	0.500	0.0418	0.0376	0.0255	0.0285
0.42	1.000	0.0248	0.0218	0.0152	0.0166
0.85	2.050	0.0073	0.0045	0.0018	0.0035

The calculations were for speeds of 2 and 8 m s^{-1} ($Re_L = 4.8 \times 10^6$ and 1.9×10^7 , respectively) in an environment with the viscosity and density of sea water at 21°C and for different transition locations.

Transition locations at distances (x) along the length (L) of the ellipsoid of 0.125, 0.5 and 1.0 m correspond to positions on a dolphin near the apex of the dolphin's melon and the anterior insertions of the pectoral and dorsal fins, respectively.

Re_L , Reynolds number based on ellipsoid length.

demarcates the edge of the flow volume where bioluminescence may occur (Fig. 5C). For both speeds, the numerical simulation showed that the $\tau \approx 0.1 \text{ N m}^{-2}$ contour also serves as a good estimation of the location of the edge of the boundary layer on the ellipsoid. Flow volumes were calculated around the model for $\tau > 0.1$ and $\tau > 1.0 \text{ N m}^{-2}$, speeds of 2 and 8 m s^{-1} , and various transition locations (Table 3). The volume of flow where $\tau > 0.1 \text{ N m}^{-2}$ was always greater for the lower flow of 2 m s^{-1} , reflecting the relative thickness of the boundary layer. However, because of the increased shear at the surface, the volume of flow where $\tau > 1.0 \text{ N m}^{-2}$ was always greater at the higher flow of 8 m s^{-1} .

Dolphin flow visualization

Video images of the dolphin NAY gliding at a speed of approximately 1 m s^{-1} beside the boat consistently showed most of the body brightly illuminated by a thin shroud of bioluminescence (Fig. 6A). Trails of bioluminescence were observed in the wakes behind the dolphin's dorsal fin, pectoral fins and flukes. When NAY executed a curved trajectory so that the flow of water moved from left to right across the body, a conspicuous region of bright bioluminescence streamed off the leeward side of the rostrum (Fig. 6B). During this maneuver, lines of bioluminescence extended from the tips of the pectoral and dorsal fins (Fig. 6B).

Another distinguishable feature shared by most of the images of NAY was the conspicuous lack of bioluminescence observed around the melon and the leading edges of the dorsal and pectoral fins (Fig. 6A–C). When a 6.5 cm diameter by 2 cm high cylinder was attached to the pectoral fin, flow separation resulted in a dramatic increase in bioluminescence (Fig. 6C,D). On subsequent nights, when experiments were repeated closer to shore light and beneath a crescent moon, the quality of the bioluminescent images was greatly degraded.

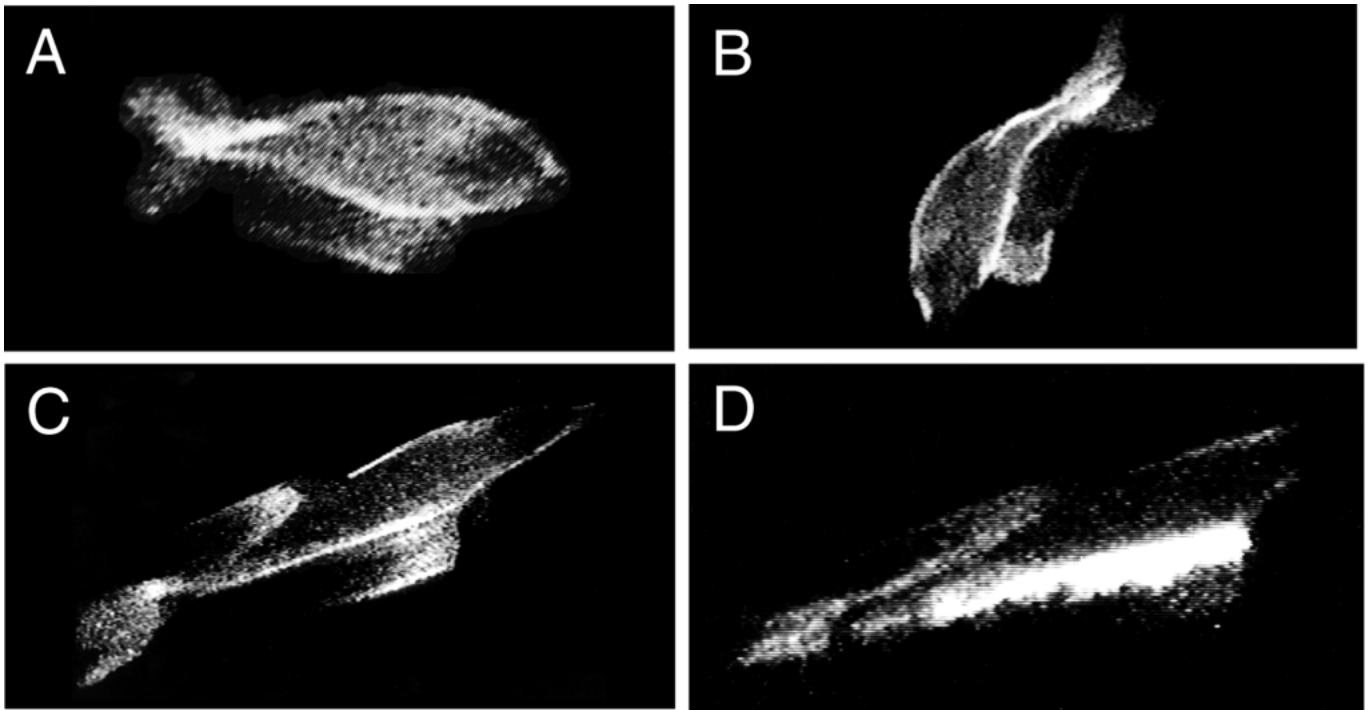


Fig. 6. Bioluminescence images of the 2.67 m long dolphin NAY gliding alongside a boat moving at approximately 0.1 m s^{-1} . Each image represents a single video frame. (A) Bioluminescence covered most of the body, with the exception of the melon. (B) Turning to his left accentuated bioluminescence on the right side of the rostrum, where the flow was separating, and within contrails streaming off the dorsal and pectoral fins. (C,D) Effect of flow separation by a 6.5 cm diameter by 2 cm high cylinder fastened to the pectoral fin. In D, a dramatic increase in bioluminescence occurred in the separated wake of the cylinder. In all images, there was reduced bioluminescence on the melon and leading edges of the fins.

The FLP experiments, performed under more controlled conditions in an enclosed pen, permitted closer inspection of the bioluminescence stimulated on the dolphin surface. A representative composite of six overlapping video frames of FLP gliding at a speed of approximately 2.2 m s^{-1} showed a pattern of flow-stimulated bioluminescence similar to that recorded for NAY. Bioluminescence occurred over much of the body (Fig. 7A), with a bright trail of bioluminescence from the dorsal fin. As with NAY, the smallest amounts of bioluminescence were observed around the positions of the rostrum, the melon and the leading edge of the dorsal fin. Increased levels of bioluminescence appeared near the blowhole, which formed a depression approximately 0.5 cm deep (Fig. 7B). Bioluminescence behind the blowhole spread out along the dolphin surface in an inverted V-shaped pattern. A Velcro strap placed at the midpoint of the dolphin's rostrum, to force transition from laminar to turbulent flow, resulted in a dramatic increase in stimulated light immediately downstream (Fig. 7C). To study the effect of flow separation, a blunt-faced object resembling an inverted cup was placed over the animal's rostrum. Bioluminescence showed flow separating around the edges of the flat surface and forming vortical structures that were advected along the dolphin's body (Fig. 7D). The swimming patterns of small fish avoiding the dolphin produced sinusoidal 'signatures' of flow-induced bioluminescence (Fig. 7A–C).

Discussion

Effect of organism concentration

Laboratory flow-visualization studies indicated that, once critical levels of flow stimulation and cell concentration were exceeded, the quality of bioluminescence images recorded with the video camera became less dependent on the dinoflagellate cell concentration. Field recordings during conditions with bioluminescence potentials greater than approximately $4 \times 10^{12} \text{ photons l}^{-1}$ were adequate to ensure good bioluminescent images (see Table 1). To achieve these levels of bioluminescence, the concentration of luminescent dinoflagellates common to San Diego Bay must be of the order of several thousand per liter. During an extensive time series study conducted in San Diego Bay from the summer of 1992 to the winter of 1994 (Lapota *et al.* 1994), concentrations of luminescent dinoflagellates reached or exceeded this level approximately 20% of the time. High concentrations occurred mostly during the summer months.

Organism response

The flow-induced threshold for the stimulation of bioluminescence for the mixed plankton samples consistently occurred in laminar flow at $\tau_{\text{wall}} = 0.1 \text{ N m}^{-2}$. This threshold level was essentially identical to measurements made over several years using the same apparatus with mixed plankton samples from San Diego Bay (Rohr *et al.* 1997). A similar

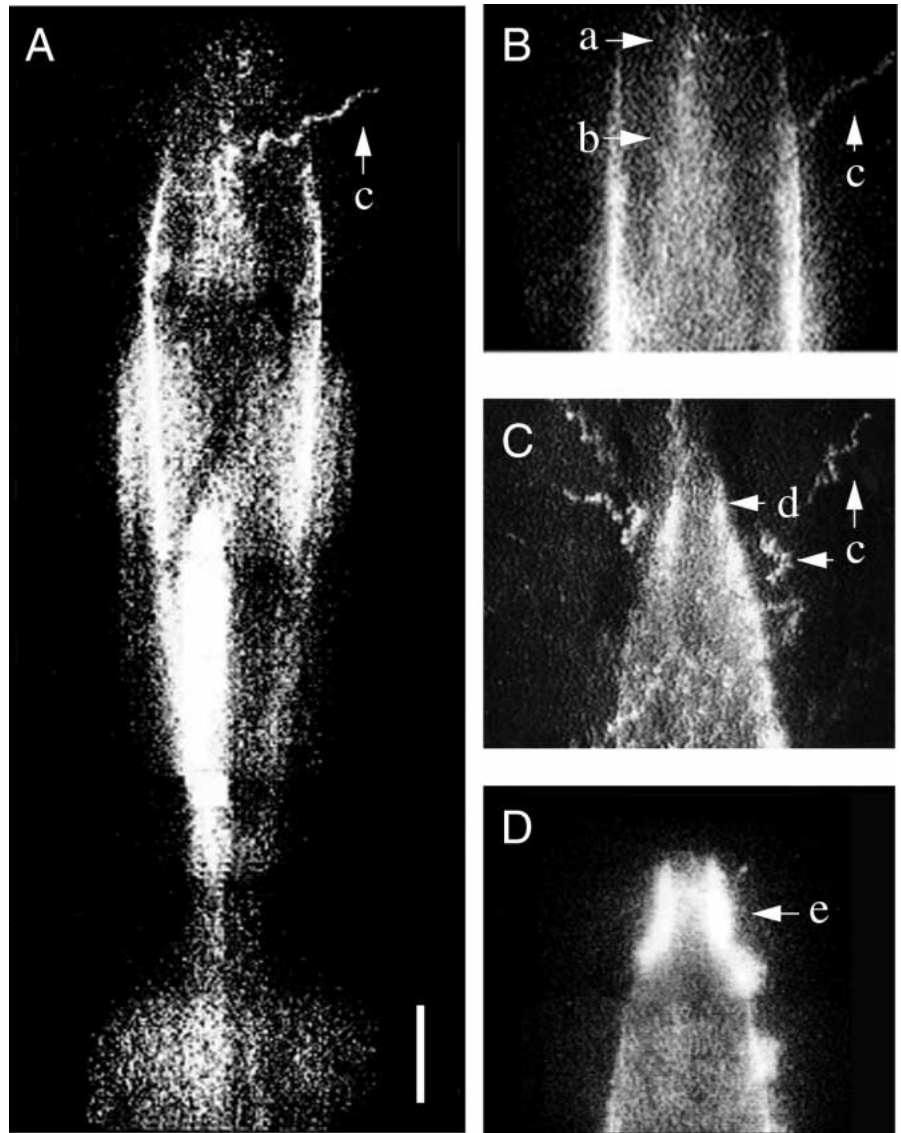


Fig. 7. Bioluminescence images of a dorsal view of the dolphin FLP gliding beneath the video camera at approximately 2.2 m s^{-1} . (A) Composite of six video frames showing the bioluminescence pattern over the entire body. (B) Single frame viewing the region behind the blowhole, showing an inverted V-shaped pattern (b) of bioluminescence downstream of the blowhole (a). (C) Single frame of the anterior end showing the increase in bioluminescence (d) resulting from a strap placed across the rostrum. (D) Single frame of the same view as in C showing bioluminescence stimulated by flow separation (e) due to an inverted cup placed on the rostrum. Sinusoidal trajectories (c) in A, B and C are due to plankton bioluminescence stimulated by the swimming movements of small fish avoiding the dolphin. Scale bar in A, 0.2 m.

threshold for bioluminescence has been measured for Sargasso Sea mixed plankton and unialgal cultures of the dinoflagellates *Lingulodinium polyedrum* and *Pyrocystis noctiluca* (Latz *et al.* 1994). Latz *et al.* (1994) used Couette flow, established in the gap between concentric cylinders with the outer cylinder rotating and the inner one held stationary, which is characterized by constant shear. In addition to these fully developed flow fields, the calculated response threshold of unialgal cultures of *L. polyedrum* stimulated in the developing flow field around a falling sphere occurred at a similar shear stress level (M. I. Latz and J. F. Case, unpublished observations). The stimulation of luminescent organisms in laminar flow is consistent with observed occurrences of bioluminescence (Latz *et al.* 1994) and its function as an anti-predation strategy (Morin, 1983).

Maximum flash intensity of individual cells exhibited a graded response, increasing from threshold at $\tau_{\text{wall}}=0.1 \text{ N m}^{-2}$ to a sustained maximum response for $\tau_{\text{wall}} \geq 1 \text{ N m}^{-2}$, regardless

of whether the flow was laminar or turbulent. This response pattern is also consistent with that found for mixed plankton samples collected from San Diego Bay (Rohr *et al.* 1997). Evidently, the length scales and intensity of turbulence are unimportant in eliciting additional bioluminescence from individual organisms.

Although pipe flow experiments were not carried out during the open-ocean NAY experiment, measurements obtained from the same pipe flow apparatus have been reported for unialgal cultures of *L. polyedrum* at similar concentrations (Latz *et al.* 1995). Under these simulated red-tide conditions, the response threshold occurred again in laminar flow at $\tau_{\text{wall}} \approx 0.2 \text{ N m}^{-2}$, and maximum bioluminescence exhibited no significant change in intensity for $\tau_{\text{wall}} \geq 1 \text{ N m}^{-2}$. These data suggest that plankton abundance in the pipe flow experiments affected only the absolute intensity of bioluminescence, but not the sensitivity of the organisms to shear stress.

There was no evidence that upstream depletion of

bioluminescence significantly affected downstream response patterns. Laboratory pipe flow studies (Rohr *et al.* 1997; present study) demonstrate that flashes occur everywhere along the 1 m length of the pipe. Using a viewing chamber attached to the end of a hose, Losee and Lapota (1981) measured only a 22 % reduction in bioluminescence over a distance of 114 m. The additional flow agitation provided by the same viewing chamber attached to the end of a 3 m pipe, where τ_{wall} was approximately 100 N m^{-2} , increased bioluminescence by five- to tenfold (J. Rohr, unpublished data). These observations indicate that upstream conditions stimulated only a small fraction of the total bioluminescence potential.

In the flow around a dolphin, the additional flow agitation associated with transition and separation is expected to be even less affected by upstream depletion because of the entrainment of fresh organisms. For example, a cylinder attached to the pectoral fin of NAY resulted in bright bioluminescence due to flow separation, even though low levels of bioluminescence were present in the absence of the cylinder. Therefore, the low probability of bioluminescence stimulation, coupled with the minimal stimulation of bioluminescence at the anterior (upstream) portion of the dolphin body and the possibility of entraining fresh fluid into regions of suprathreshold shear, suggests that a significant reservoir of bioluminescent potential exists at any point on the dolphin's body.

There was also no observable effect on the bioluminescence patterns due to the 20 ms response latency of the organisms. The laboratory and field experiments involving flow separation and laminar-to-turbulent transition clearly show bioluminescence occurring immediately behind the object affecting the flow. This is presumably due to the short response latency of the dinoflagellates and their slower advection in the boundary layer.

Interpreting dolphin-stimulated bioluminescence

While the dark-adapted human eye and the ISIT video camera are very sensitive to small changes in source brightness, they are both limited in their ability to quantify intensity levels. The human eye senses intensity levels as changes in brightness. The perception of brightness is a function not only of the intensity of light falling on a given region of the retina but also of the intensity of the light to which that region of the retina has recently been exposed and the intensity of light illuminating other regions of the retina (Rock, 1984; Gregory, 1990). Determining absolute levels of *in situ* bioluminescence with an ISIT video camera is also inherently problematic, because unsaturated gray-scale values are required for accurate photon calibration, and bright video images are best achieved with pixel elements with saturated gray-scale values. Nevertheless, under suitably dark conditions, changes in bioluminescence intensity are often apparent both to the eye and to the camera.

The numerical simulations, together with the pipe flow results, indicate that even under the most conservative conditions of laminar flow, cruising speeds and a rigid body, suprathreshold levels of flow stimuli for bioluminescence

should be present everywhere on the dolphin. Because the maximum response of individual organisms was unchanged for $\tau_{\text{wall}} \geq 1.0 \text{ N m}^{-2}$, regardless of whether the flow was laminar or turbulent, it is hypothesized that the thickness of the boundary layer will be the primary determinant of the number of luminescent organisms stimulated. Consequently, where the boundary layer is relatively thin, even though high levels of flow stimulation may be present, bioluminescence will be relatively dim. Increases in boundary layer thickness associated with laminar-to-turbulent transition and flow separation should lead to conspicuous increases in bioluminescence.

Thus, the lack of bioluminescence on the forward portion of the dolphin's melon and fins, where the surface shear stress is predicted to be highest, may have resulted from the very thin boundary layer in these regions. A similar phenomenon was observed on the forward portion of a sphere, where an increase in flow speed resulted in both a thinner boundary layer and a reduction in bioluminescence (Fig. 4A,B). The increase in bioluminescence beginning behind the dolphin blowhole is consistent with laminar-to-turbulent transition studies of surface bumps on axisymmetric bodies (Ladd, 1981). Similar disturbances produced by the projections of the eyes, wounds, nares and gill effluent of fish have been reported to cause premature transition to turbulent flow (Allen, 1961; Walters, 1962; Aleyev and Ovcharov, 1969). In addition, the corselets on spanish mackerel, tuna and skipjack, which comprise thickened scales and skin projecting slightly above the body surface near the maximum width, are hypothesized to purposely force transition in order to delay separation (Walters, 1962). Forced laminar-to-turbulent transition for dolphin models, a 6:1 ellipsoid model (Latz *et al.* 1995) and a sphere (present study) produced greater bioluminescence levels immediately behind them because of the thicker turbulent boundary layer.

When the boundary layer separated, the resulting wake became the dominant bioluminescent feature because of the significantly greater number of luminescent cells entrained and stimulated in the wake. The bright patch of bioluminescence appearing along the right side of NAY's rostrum in Fig. 6A was presumably due to flow separation caused by the animal's curved trajectory. For a straight path, it has been speculated that separation would develop at the dolphin's shoulder (Blake, 1983). Flow-visualization tests using a rigid, full-scale model of *Tursiops truncatus*, at relevant Reynolds numbers, have indicated that separation occurs just behind the dorsal fin (Purves *et al.* 1975). The present studies showed no indication of major flow separation on the gliding dolphin. Considering the extraordinarily bright bioluminescent signature produced by the wake of a relatively small cylinder attached to the pectoral fin (Fig. 6D), if flow separation had occurred at the mid-body of the dolphin, the resulting increase in bioluminescence would have been immediately apparent. Webb (1978) reached a similar conclusion on the basis of the descriptions of Steven (1950) of low levels of bioluminescent intensity in the dolphin's wake.

The 'contrails' of bioluminescence streaming from the tips of the dolphin fins were more apparent during turning than during swimming along a straight path. Even though the mechanism of flow stimulation within these tip vortices is unknown, it should be related to the magnitude of vorticity, which will increase with the pressure difference across the lifting surface. Therefore, these bioluminescent 'contrails', which have been frequently reported (Steven, 1950; Wood, 1973; Fitzgerald, 1991), should be stronger when the dolphin is turning or actively swimming. Occasionally, an apparent increase in bioluminescence was also observed along the borders of images of a dorsal view of the dolphin. This effect may simply be a result of viewing the boundary layer from the side, thereby integrating a greater volume of stimulating flow.

Even though the observations described in the present study were mostly obtained from gliding dolphins, bioluminescence patterns associated with changes in the boundary layer due to laminar-to-turbulent transition, flow separation and sufficiently energetic vortices should also occur in the case of actively swimming dolphins. For example, luminescent flow visualization can be used to test whether favorable pressure gradients associated with active swimming would cause transition to occur further along the dolphin body (Gray, 1936; Romanenko, 1995). Romanenko (1995) has suggested that the sketches of dolphin bioluminescence by McKinley and Evans (Wood, 1973) indicate transition occurring towards the middle of the animal. In addition, by visualizing fluid pathlines due to forced flow separation, it can be determined whether flow follows the orientation of the dermal ridges of the dolphin (Purves *et al.* 1975; Ridgway and Carder, 1993). Finally, if vortices generated along the body and in the wake of a swimming dolphin or fish (Triantafyllou *et al.* 1993; Triantafyllou and Triantafyllou, 1995) are sufficiently energetic, they may also be visualized through bioluminescence. Thus, luminescent flow visualization of actively swimming animals may help to identify flow features associated with propulsive efficiency.

Observations and interpretations of flow-induced bioluminescence are affected by many factors, including the assemblage and concentration of luminescent organisms, their response to hydrodynamic stimulation, the flow field within which they are stimulated and limitations of the recording instrumentation. Nonetheless, the present results suggest that, when the plankton bioluminescence potential is adequate and ambient lighting conditions are suitable, the use of bioluminescence as a flow diagnostic tool in field applications with large marine animals has excellent potential. Because bioluminescent plankton are a ubiquitous component of the dolphin's natural environment and many species can be cultured in the laboratory, this method can be applied in both laboratory and field settings to test a variety of questions related to the swimming mechanics of aquatic animals.

The present study establishes a framework for interpreting the hydrodynamic basis of flow-induced bioluminescence. The results necessitate a reassessment of previous assumptions (Hill, 1950; Steven, 1950; Wood, 1973; Fitzgerald, 1991;

Ridgway and Carder, 1993) about dolphin-stimulated bioluminescence. For example, it can no longer be assumed that the presence of bioluminescence is necessarily indicative of turbulent flow, nor is an observed lack of bioluminescence necessarily indicative of subthreshold levels of flow stimuli. The present numerical and experimental studies indicate that, even under the most conservative conditions of laminar flow, cruising speed and gliding motion, shear stress levels on the dolphin's body are everywhere greater than the threshold for bioluminescence stimulation. Therefore, regardless of whether flow is laminar or turbulent, bioluminescence stimulation is expected to occur throughout the dolphin boundary layer. The present data suggest that changes in the boundary layer thickness account for the observed patterns of flow-induced bioluminescence.

The authors thank A. Huvad for analyzing the plankton samples, D. Ladd for help with the numerical simulations, the crew of *La Salsa* for assistance in the field studies, and trainers S. Meck and B. Right for assistance with the dolphins. Dolphins were maintained by the Navy Marine Mammal Program under applicable federal regulations and under the supervision of an attending veterinarian and an institutional animal care and use committee. We thank L. E. McKinley for making available to us his drawings of dolphins swimming through bioluminescent waters, Begell House Inc. for permission to reproduce Fig. 7A, which originally appeared in *Flow Visualization VII: Proceedings of the Seventh International Symposium on Flow Visualization* (ed. J. P. Crowder), and Cordon Art B.V. for permission to reproduce the sketch by M. C. Escher. We would also like to acknowledge T. Cranford, J. Hoyt, L. Quigley, S. Ridgway and F. Fish for reviewing the manuscript and making many helpful suggestions. This investigation was supported by J. Fein of the Office of Naval Research, A. Gordon of SPAWARSYSCEN and grant N00014-95-1-0001 from the Office of Naval Research (to M.I.L.).

References

- ALEYEV, Y. G. AND OVCHAROV, O. P. (1969). Development of vortex forming processes and nature of the boundary layer with movement of fish. *Zool. Zh.* **48**, 781–790.
- ALLEN, W. H. (1961). Underwater flow visualization techniques. United States Naval Ordinance Test Station Technical Publication No. 2759.
- ANDERSON, D. M., NOSENCHUCK, D. M., REYNOLDS, G. T. AND WALTON, A. J. (1988). Mechanical stimulation of bioluminescence in the dinoflagellate *Gonyaulax polyedra* (Stein). *J. exp. mar. Biol. Ecol.* **122**, 277–288.
- BAKHMETEFF, B. (1936). *The Mechanics of Turbulent Flow*. Princeton, NJ: Princeton University Press.
- BIGGLEY, W. H., SWIFT, E., BUCHANAN, R. J. AND SELIGER, H. H. (1969). Stimulable and spontaneous bioluminescence in marine dinoflagellates *Pyrodinium bahamense*, *Gonyaulax polyhedra* and *Pyrocystis lunula*. *J. gen. Physiol.* **54**, 96–123.
- BITYUKOV, E. P. (1971). Bioluminescence in the wake current in the Atlantic Ocean and Mediterranean Sea. *Okean* **11**, 127–133.

- BLAKE, R. W. (1983). *Fish Locomotion*. London: Cambridge University Press.
- BOOL, F. H., KIST, J. R., LOCHER, J. L. AND WIERDA, F. (1982). *Escher His Life and Graphic Work*. Amsterdam: Abradale Press, Harry N. Abrams, Inc. Publishers.
- BUSKEY, E. J., STROM, S. AND COULTER, C. (1992). Bioluminescence of heterotrophic dinoflagellates from Texas coastal waters. *J. exp. mar. Biol. Ecol.* **159**, 37–49.
- CEBECI, T. AND SMITH, A. M. O. (1974). *Analysis of Turbulent Boundary Layers*. New York: Academic Press.
- CORNISH III, J. J. AND BOATWRIGHT, D. W. (1960). Application of full scale boundary layer measurements to drag reduction of airships. Aerophysics Department, Mississippi State University Report No. 28.
- CRAM, D. L. AND HAMPTON, I. (1976). A proposed aerial/acoustic strategy for pelagic fish stock assessment. *J. Cons. int. expl. Mer.* **37**, 91–97.
- DAVIES, J. T. (1972). *Turbulence Phenomenon*. London: Academic Press.
- ECKERT, R. (1966). Excitation and luminescence in *Noctiluca miliaris*. In *Bioluminescence in Progress* (ed. F. Johnson and Y. Haneda), pp. 269–300. Princeton, NJ: Princeton Univ. Press.
- ESAIAS, W. E., CURL, H. C. AND SELIGER, H. H. (1973). Action spectrum for a low intensity, rapid photoinhibition of mechanically stimuable bioluminescence in marine dinoflagellates *Gonyaulax catenella*, *G. acatenella* and *G. tamarensis*. *J. cell. Physiol.* **82**, 363–372.
- FISH, F. E. AND HUI, C. A. (1991). Dolphin swimming – a review. *Mammal. Rev.* **21**, 181–195.
- FITZGERALD, J. W. (1991). Artificial dolphin blubber could increase sub speed, cut noise. *Navy News undersea Tech.* **9**, 1–2.
- FITZGERALD, J. W., FITZGERALD, E. R., CAREY, W. M. AND VON WINKLE, W. A. (1995). Blubber and compliant coatings for drag reduction in water. II. Matched shear impedance for compliant layer drag reduction. *Materials Sci. Eng.* **C2**, 215–220.
- FLEISHER, K. J. AND CASE, J. F. (1995). Cephalopod predation facilitated by dinoflagellate luminescence. *Biol. Bull. mar. biol. Lab., Woods Hole* **189**, 263–271.
- GRAY, J. (1936). Studies in animal locomotion. VI. The propulsive powers of the dolphin. *J. exp. Biol.* **13**, 192–199.
- GREGORY, R. L. (1990). *Eye and Brain: The Psychology of Seeing*. Princeton, NJ: Princeton University Press.
- HARDY, A. C. (1956). *The Open Sea It's Natural History: The World of Plankton*. London: Collins.
- HARVEY, E. N. (1952). *Bioluminescence*. New York: Academic Press.
- HASTINGS, J. W. (1975). Dinoflagellate bioluminescence: Molecular mechanisms and circadian control. In *Proceedings of the First International Conference on Toxic Dinoflagellate Blooms* (ed. V. R. Lococero), pp. 235–248. Wakefield: The Massachusetts Science and Technology Foundation.
- HILL, A. V. (1950). The dimensions of animals and their muscular dynamics. *Sci. Prog.* **38**, 209–230.
- HOBSON, E. S. (1966). Visual orientation and feeding in seals and sea lions. *Nature* **214**, 326–327.
- HOBSON, E. S., MCFARLAND, W. N. AND CHESS, J. R. (1981). Crepuscular and nocturnal activities of Californian nearshore fishes, with consideration of their scotopic visual pigments and the photic environment. *Fishery Bull. Fish. Wildl. Serv. U.S.* **79**, 1–30.
- HOLMES, R. W., WILLIAMS, P. M. AND EPPLEY, R. W. (1967). Red water in La Jolla Bay 1964–1966. *Limnol. Oceanogr.* **12**, 503–512.
- IRANI, R. R. AND CALLIS, C. F. (1973). *Particle Size: Measurement, Interpretation and Application*. New York: Wiley.
- KELLY, M. G. (1968). *Oceanic Bioluminescence and the Ecology of Dinoflagellates*. Boston: Harvard University. 186pp.
- KELLY, M. G. AND TETT, P. (1978). Bioluminescence in the ocean. In *Bioluminescence in Action* (ed. P. J. Herring), pp. 399–417. New York: Academic Press.
- KIMOR, B. (1983). Seasonal and bathymetric distribution of thecate and nonthecate dinoflagellates off La Jolla, California. *CalCOFI Rep.* **22**, 126–134.
- LADD, D. M. (1981). The effect of surface bumps on the drag of an axisymmetric body. Naval Ocean Systems Center Technical Note No. 1069.
- LADD, D. M. AND HENDRICKS, E. W. (1985). The effect of background particulates on the delayed transition of a heated 9:1 ellipsoid. *Exp. Fluids* **3**, 113–119.
- LANG, T. G. (1975). Speed, power and drag measurements of dolphins and porpoises. In *Swimming and Flying in Nature* (ed. T. W. Wu, C. J. Borkaw and C. Brennen), pp. 553–571. New York: Plenum Press.
- LANG, T. G. AND DAYBELL, D. A. (1963). Porpoise performance tests in a seawater tank. Naval Ordinance Test Station Technical Publication No. 3063.
- LANG, T. G. AND NORRIS, K. N. (1966). Swimming speed of a Pacific bottlenose porpoise. *Science* **151**, 588–590.
- LAPOTA, D., GEIGER, M. L., STIFFEY, A. V., ROSENBERGER, D. E. AND YOUNG, D. K. (1989). Correlations of planktonic bioluminescence with other oceanographic parameters from a Norwegian fjord. *Mar. Ecol. Prog. Ser.* **55**, 217–227.
- LAPOTA, D., PADEN, S., DUCKWORTH, D., ROSENBERGER, D. E. AND CASE, J. F. (1994). Coastal and oceanic bioluminescence trends in the southern California bight using Moordex bathyphotometers. In *Bioluminescence and Chemiluminescence: Fundamentals and Applied Aspects* (ed. A. K. Campbell, L. J. Kricka and P. E. Stanley), pp. 127–130. New York: John Wiley & Sons.
- LATZ, M. I., CASE, J. F. AND GRAN, R. L. (1994). Excitation of bioluminescence by laminar fluid shear associated with simple Couette flow. *Limnol. Oceanogr.* **39**, 1424–1439.
- LATZ, M. I. AND LEE, A. O. (1995). Spontaneous and stimulated bioluminescence of the dinoflagellate *Ceratocorys horrida* (Peridinales). *J. Phycol.* **31**, 120–132.
- LATZ, M. I., ROHR, J. AND CASE, J. F. (1995). Description of a novel flow visualization technique using bioluminescent marine plankton. In *Flow Visualization*, vol. VII (ed. J. P. Crowder), pp. 28–33. New York: Begell House, Inc.
- LAUFER, J. (1954). The structure of turbulence in fully developed pipe flow. National Advisory Committee for Aeronautics Technical Report No. 1174.
- LOSEE, J. R. AND LAPOTA, D. (1981). Bioluminescence measurements in the Atlantic and Pacific. In *Bioluminescence Current Perspectives* (ed. K. H. Nealson), pp. 143–152. Minneapolis: Burgess Publishing Co.
- LYNCH, D. K. AND LIVINGSTON, W. (1995). *Color and Light in Nature*. Cambridge: Cambridge University Press.
- LYTHGOE, J. N. (1972). The adaptation of visual pigments to the photic environment. In *Handbook of Sensory Physiology*, vol. VII (ed. H. J. A. Dartnall), pp. 566–603. New York: Springer-Verlag.
- MCCUTCHEN, C. W. (1976). Flow visualization with stereo shadowgraphs of stratified flow. *J. exp. Biol.* **65**, 11–20.
- MENSINGER, A. F. AND CASE, J. F. (1992). Dinoflagellate luminescence increases susceptibility of zooplankton to teleost predation. *Mar. Biol.* **112**, 207–210.

- MORIN, J. G. (1983). Coastal bioluminescence: patterns and functions. *Bull. mar. Sci.* **33**, 787–817.
- MURPHY, J. S. (1954). The separation of axially-symmetric turbulent boundary layers. Part I. Preliminary experimental results on several bodies in incompressible flows. Part II. Detailed measurements in the boundary layers on several slender bodies in incompressible flow. Douglas Aircraft Company Report No. ES 17513.
- NORRIS, K. S. (1965). Trained porpoise released in the open sea. *Science* **147**, 1048–1050.
- PURVES, P. E., DUDOK VAN HEEL, W. H. AND JONK, A. (1975). Locomotion in dolphins. Part I. Hydrodynamic experiments on a model of the bottle-nosed dolphin, *Tursiops truncatus* (Mont.). *Aquat. Mam.* **3**, 5–31.
- RIDGWAY, S. H. AND CARDER, D. H. (1993). Features of dolphin skin with potential hydrodynamic importance. *IEEE Eng. Med. Biol. Mag.* September, 83–88.
- ROCK, I. (1984). *Perception*. New York: Scientific American Library, Scientific American Books, Inc., distributed by W. H. Freeman and Company.
- ROHR, J., LOSEE, J. AND ANDERSON, G. (1994). The response of bioluminescent organisms to fully developed pipe flow. Naval Command, Control and Ocean Surveillance Center, RDT&E Div. Technical Report No. 1360.
- ROHR, J., LOSEE, J. AND HOYT, J. (1990). Stimulation of bioluminescence by turbulent pipe flow. *Deep-Sea Res.* **37**, 1639–1646.
- ROHR, J. J., ALLEN, J., LOSEE, J. AND LATZ, M. I. (1997). The use of bioluminescence as a flow diagnostic. *Physiol. Lett. A* **228**, 408–416.
- ROITHMAYR, C. M. (1970). Airborne low-light sensor detects luminescing fish schools at night. *Commer. Fish. Rev.* **32**, 42–51.
- ROMANENKO, E. V. (1995). Swimming of dolphins: experiments and modelling. In *Biological Fluid Dynamics* (ed. C. P. Ellington and T. J. Pedley), pp. 21–33. Cambridge: The Company of Biologists Limited.
- ROSEN, M. W. (1963). Flow visualization experiments with a dolphin. United States Naval Ordinance Test Station Technical Publication No. 3065.
- SCHLICHTING, H. (1979). *Boundary-layer Theory*. New York: McGraw-Hill Inc.
- SMITH, A. M. O. AND GAMBERONI, N. (1956). Transition, pressure gradient and stability theory. *Proc. Int. Congr. appl. Mech.* **4**, 234.
- STAPLES, R. F. (1966). The distribution and characteristics of surface bioluminescence in the oceans. Naval Oceanographic Office Technical Report No. 184.
- STEVEN, G. A. (1950). Swimming of dolphins. *Sci. Prog.* **38**, 524–525.
- SWEENEY, B. M. (1963). Bioluminescent dinoflagellates. *Biol. Bull. mar. biol. Lab., Woods Hole* **125**, 177–181.
- SWEENEY, B. M. (1981). Variations in the bioluminescence per cell in dinoflagellates. In *Bioluminescence: Current Perspectives* (ed. K. Neelson), pp. 52–63. Minneapolis: Burgess Publishing Co.
- TARASOV, N. I. (1956). Marine luminescence. Naval Oceanographic Office Report No. NOO T-21.
- TETT, P. B. AND KELLY, M. G. (1973). Marine bioluminescence. *Oceanogr. mar. Biol. A. Rev.* **11**, 89–73.
- THOMPSON, D. (1971). *On Growth and Form*. Cambridge: Cambridge University Press.
- TRIAANTAFYLLOU, G. S., TRIAANTAFYLLOU, M. S. AND GROSENBAUGH, M. A. (1993). Optimal thrust development in oscillating foils with application to fish propulsion. *J. Fluids Struct.* **7**, 205–224.
- TRIAANTAFYLLOU, M. S. AND TRIAANTAFYLLOU, G. S. (1995). An efficient swimming machine. *Scient. Am.* **272**, 64–70.
- VAN INGEN, J. L. (1956). A suggested semi-empirical method for the calculation of the boundary layer transition region. Department of Aeronautics Engineering Technical University V.T.H. No. 74.
- WALTERS, V. (1962). Body form and swimming performance in the scombroid fishes. *Am. Zool.* **2**, 143–149.
- WEBB, P. W. (1978). Hydrodynamics: nonscombroid fish. In *Fish Physiology*, vol. VII (ed. W. S. Hoar and D. J. Randall), pp. 189–237. New York: Academic Press.
- WIDDER, E. A. AND CASE, J. F. (1981). Bioluminescence excitation in a dinoflagellate. In *Bioluminescence Current Perspectives* (ed. K. H. Neelson), pp. 125–132. Minneapolis: Burgess Publishing Co.
- WIDDER, E. A., CASE, J. F., BERNSTEIN, S. A., MACINTYRE, S., LOWENSTINE, M. R., BOWLBY, M. R. AND COOK, D. P. (1993). A new large volume bioluminescence bathyphotometer with defined turbulence excitation. *Deep-Sea Res.* **40**, 607–627.
- WILLIAMS, T. M., FRIEDL, W. A. AND HAUN, J. E. (1993). The physiology of bottlenose dolphins (*Tursiops truncatus*): heart rate, metabolic rate and plasma lactate concentration during exercise. *J. exp. Biol.* **179**, 31–46.
- WILLIAMS, T. M. AND KOOYMAN, G. L. (1985). Swimming performance and hydrodynamic characteristics of harbor seals *Phoca vitulina*. *Physiol. Zool.* **58**, 576–589.
- WOOD, F. G. (1973). *Marine Mammals and Man*. New York: R. B. Luce, Inc.
- YOUNG, A. D. (1989). *Boundary Layers*. Oxford: BSP Professional Books.